

# OXYGEN ABUNDANCES IN METAL-POOR STARS ( $-2.2 < [\text{Fe}/\text{H}] < -1.2$ ) FROM INFRARED OH LINES

Jorge Meléndez <sup>1</sup> and Beatriz Barbuy

*Universidade de São Paulo, IAG, Dept. de Astronomia, CP 3386, São Paulo 01060-970, Brazil*

*E-mail: jorge@iagusp.usp.br, barbuy@orion.iagusp.usp.br*

and

François Spite

*Observatoire de Paris-Meudon, DASGAL, F-92195 Meudon Cedex, France*

*E-mail: Francois.Spite@obspm.fr*

## ABSTRACT

Infrared OH lines at 1.55 - 1.56  $\mu\text{m}$  in the H-band were obtained with the Phoenix high-resolution spectrograph at the 2.1m telescope of the Kitt Peak National Observatory for a sample of 14 metal-poor stars.

Detailed analyses of the sample stars have been carried out, deriving stellar parameters based on two methods: (a) spectroscopic parameters; (b) IRFM effective temperatures, trigonometric gravities and metallicities from Fe II lines. The Fe I lines present in the H-band region observed showed to be well fitted by the stellar parameters within  $\Delta[\text{Fe}/\text{H}] \leq 0.15$  dex.

The oxygen abundances were derived from fits of spectrum synthesis calculations to the infrared OH lines. CO lines in the H- and K-bands were obtained for a subsample in order to determine their carbon abundances.

Adopting the spectroscopic parameters a mean oxygen-to-iron ratio of  $[\text{O}/\text{Fe}] \approx +0.52$  is obtained, whereas using the IRFM temperatures, Hipparcos gravities and  $[\text{Fe II}/\text{H}]$ ,  $[\text{O}/\text{Fe}] \approx +0.25$  is found. A mean of the two methods gives a final value of  $[\text{O}/\text{Fe}] \approx +0.4$  for the metallicity range  $-2.2 < [\text{Fe}/\text{H}] < -1.2$  of the sample metal-poor stars.

---

<sup>1</sup>Visiting Astronomer, Kitt Peak National Observatory, National Optical Astronomy Observatories, which is operated by the Association of Universities for Research in Astronomy, Inc. (AURA) under cooperative agreement with the National Science Foundation

## 1. Introduction

Oxygen abundances in metal-poor stars are a key result for constraining several important issues such as the age of globular clusters (VandenBerg 1985, VandenBerg et al. 2000), models of cosmic ray spallation (Walker et al. 1993; Fields & Olive 1999; Kneller, Steigman & Walker 2001), chemical evolution models in the early phases of the Galaxy evolution (Chiappini et al. 1999, hereafter CMBN99; Pagel & Tautvaišienė 1995, hereafter PT95) and nucleosynthesis ejecta of massive stars (Thielemann, Nomoto & Hashimoto 1996, hereafter TNH96; Woosley & Weaver 1995, hereafter WW95).

Oxygen is a major tracer of chemical evolution, since it is a bona fide primary element ejected by massive stars. The oxygen-to-iron ratio is a measure of SNII/SNI rates along time, and can be used to characterize fast chemical enrichment ( $[O/Fe] > 0$ ) such as in the halo of our Galaxy.

There is agreement in the literature concerning an overabundance of oxygen relative to iron in metal-poor stars. This result was first established by Conti et al. (1967) and Sneden et al. (1979). However there is no agreement on the overabundance value itself. The reasons for the discrepancies come from the fact that only four sets of lines can be used to derive oxygen abundances in metal-poor stars: (i) the forbidden  $[O\ I]\lambda 6300.31, \lambda 6363.79$  Å lines measurable in giants of  $[Fe/H] > -3.0$ ; (ii) the permitted  $O\ I\lambda 7771.96, 7774.18$  and  $7775.40$  Å lines measurable in dwarfs and subgiants; (iii) the ultraviolet (UV) OH lines ( $A^2\Sigma-X^2\Pi$  electronic transition); (iv) the infrared (IR) OH lines ( $X^2\Pi$  vibration-rotation transition).

Therefore there are only a few lines available, and in most cases the different lines are not present in the same stars.  $O\ I$  permitted lines give systematically higher values than the  $[O\ I]$  forbidden lines. The problems with the different lines can be summarized as follows.

(i) The reliability of the forbidden lines  $[O\ I]$  present in giants stems from the fact that the transition involves a metastable level, collisionally controlled, therefore not directly subject to non-LTE effects (see Kiselman 2001a,b; Lambert 2001). Values of  $[O/Fe] \approx +0.4$  to  $+0.6$  down to  $[Fe/H] \approx -3.0$  are obtained (e.g. Gratton & Ortolani 1986; Barbuy 1988; Sneden et al. 1991; Spiesman & Wallerstein 1991; Kraft et al. 1992; Shetrone 1996; Carretta et

al. 2000; Gratton et al. 2000; Westin et al. 2000; Asplund 2001a,b; Cayrel et al. 2001a; Nissen et al. 2001; Sneden & Primas 2001a,b); below  $[Fe/H] < -3.0$  the oxygen forbidden lines are too faint.

(ii) the permitted lines of the  $O\ I$  triplet present in dwarfs, give  $[O/Fe] \approx +1.0$  at  $[Fe/H] \approx -3.0$  (e.g. Abia & Rebolo 1989; Cavallo, Pilachowski & Rebolo 1997; Mishenina et al. 2000). However the permitted lines of high excitation potential seem to be subject to overenhancements, partly due to non-LTE (Kiselman 2001a,b) and partly to uncertainties in the deep layers of model atmospheres, as is also the case of  $C\ I$  lines of high excitation potential (Tomkin et al. 1992). An evidence of this 'artificial' overenhancement was demonstrated through the study of both forbidden and permitted lines in some samples of stars, and they give different results for a given star (Spite & Spite 1991; Fulbright & Kraft 1999).

King (1993) claimed that by adopting a hotter effective temperature  $T_{eff}$  scale and depending on the models, it is possible to obtain  $[O/Fe] \approx +0.5$  for halo dwarfs derived from the permitted lines, comparable to those obtained from the forbidden lines for giants. Carretta et al. (2000) obtained the same results, also adopting a higher  $T_{eff}$  scale and non-LTE corrections applied to the permitted lines. King (2000) applied NLTE corrections on the stellar parameters  $\log g$  and  $[Fe/H]$ , and obtained  $[O/Fe] \approx 0.6$  at  $[Fe/H] \approx -3.0$ .

It is important to note also that detailed non-LTE calculations cannot reproduce the solar permitted lines (Kiselman & Nordlund 1995; Kiselman 2001a,b).

(iii) Recently, new data on the UV OH lines (Israelian, García López & Rebolo 1998, hereafter IGR98; Boesgaard et al. 1999, hereafter BKDV99) appear to give high oxygen abundances, in agreement with the permitted lines, although these lines had been already studied in the past by Bessell, Sutherland & Ruan (1991) and Nissen et al. (1994) who found  $[O/Fe] \approx +0.5/+0.6$  and  $+0.6$  respectively, in better agreement with the forbidden lines. It is clear that determinations of oxygen abundances from UV OH lines are affected however at least by different questionable fittings of molecular oscillator strengths to the solar spectrum (see Sect. 4).

(iv) The IR OH transitions were considered as one of the more reliable oxygen abundance indicators by Grevesse & Sauval (1994). Despite this, essentially no oxygen abundance determinations in metal-poor stars using these lines are available, except for the pioneer-

ing work by Balachandran & Carney (1996, hereafter BC96) for the star HD 103095 for which  $[\text{Fe}/\text{H}] = -1.22$  and  $[\text{O}/\text{Fe}] = 0.29$  were derived. Balachandran et al. (2001a,b) presented new oxygen abundance determinations from IR OH lines; their preliminary  $[\text{O}/\text{Fe}]$  values show agreement with those derived from  $[\text{OI}]$  lines.

In the present work we use infrared OH lines in the region  $1.55 - 1.56 \mu\text{m}$ , in order to derive oxygen-to-iron ratios for a sample of 14 metal-poor stars.

In Sect. 2 the observations are presented. In Sect. 3 the detailed analyses are described. In Sect. 4 some considerations on UV OH lines are given. In Sect. 5 the results from IR OH lines are discussed and in Sect. 6 conclusions are drawn.

## 2. Observations

### 2.1. Data Acquisition

High-resolution infrared spectra were obtained from images taken at the 2.1 m telescope of the Kitt Peak National Observatory using the Phoenix spectrograph. Phoenix is described in detail by Hinkle et al. (1998). This instrument uses a cryogenic échelle grating to achieve FWHM resolutions of 50,000 to 75,000, depending on slit width. Order separating filters are used to isolate individual échelle orders (the instrument is not cross dispersed) in the  $1 - 5 \mu\text{m}$  region. The detector is an Aladdin 512x1024 InSb array, covering  $1500 \text{ km s}^{-1}$  in wavelength.

Each star was observed at least at two slit positions with the same integration time, with offsets of  $15''$  between integrations, obtaining two spectra in different positions on the detector. The sky background is eliminated by subtracting the first exposure from the sky obtained in the second one at that position in the detector, and the same method for the second exposure and sky from the first one. About 30 flatfields and darks were taken, with exposure times of 15 and 20 s for the H- and K-band, respectively. Most of the data were gathered in the H-band, centered at  $1.5555 \mu\text{m}$ , with a spectral coverage of  $75 \text{ \AA}$ . This region was chosen because it has several unblended vibration-rotation lines of OH, and also because it is almost free from disturbing telluric features. For a few stars for which no carbon abundance determinations were available in the literature, we observed the CO lines present at  $2.3 \mu\text{m}$ , in order to determine their carbon abundances, since a fraction of the oxygen is tied up in CO molecules. The observations of OH lines in the

H-band were obtained using the 3-pixel slit, achieving a FWHM resolution of 60,000. The K-band observations of CO lines were done using the 4-pixel slit, with a FWHM resolution of 50,000. For wavelength calibration purposes we have observed the Moon, obtaining reflected solar spectra. Hot stars with high  $vsini$  were observed to check for the presence of telluric lines in both the H and K-band spectra. The log of observations is given in Table 1.

### 2.2. Data reduction

The data were reduced following the standard Phoenix procedures <sup>2</sup>, with some improvements, in order to obtain resulting spectra of higher quality.

The flatfield and dark frames were combined, and the combined dark frame was subtracted from the combined flatfield frame. A mask of bad pixels (both dead and hot pixels) was created and these pixels were reconstructed by interpolation. A response image was created by fitting a surface to the resulting flatfield. The bad pixels were reconstructed by interpolation using the bad pixel mask. The spectra were then divided by the response image and one-dimensional spectra were extracted (cosmic rays were eliminated in the process).

The wavelength calibration of the H-band spectra was done using the reflected solar spectrum and employing the list of atomic lines by Meléndez & Barbuy (1999). The solar features were identified using the solar Atlas of Livingston & Wallace (1991). This procedure provided a calibration with an r.m.s. error of  $\Delta\lambda/\lambda \approx 10^{-6}$ , compatible with an error of  $0.02 \text{ \AA}$  in the wavelengths of our line list. On the first night (Sep. 21st) the Moon was not observed; instead the giant HR 1481 of spectral type K1.5III was observed (same spectral type of Arcturus) and for spectra taken on Sep. 21st we used this giant to carry out the wavelength calibration, again employing the wavelengths by Meléndez & Barbuy (1999) but in this case the identifications were done using the Atlas of Arcturus by Hinkle, Wallace & Livingstone (1995). For comparison purposes we observed a metal-poor star (HD 37828) in the two nights and compared the wavelength calibrations obtained using either the Moon or the giant spectra. We found both dispersion solutions in good agreement. For the K-band spectra we have used telluric features for wavelength calibration. Telluric spectra were obtained by

<sup>2</sup><ftp://iraf.noao.edu/iraf/misc/phoenix.readme>

observing hot stars with high  $vsini$ . Wavelengths of telluric lines were measured in the Atlas of Livingston & Wallace (1991). We obtained a r.m.s. error of  $\Delta\lambda/\lambda \approx 2 \times 10^{-6}$ . Finally, multiple exposures along the slit were co-added, and the resulting spectra have high S/N ratio (column 5 of Table 1), typically S/N  $\approx 100\text{--}200$ , estimated from continuum regions. The normalized H-band spectrum of HD 187111 is shown in Figure 1.

In order to compare our calculations of oxygen abundances to those by BC96, we have extracted the spectrum of HD 103095 from their publication, using the Dexter utility <sup>3</sup> (see Sect. 5).

### 3. DETAILED ANALYSIS

The sample consists of 3 dwarfs, 3 subgiants and 9 giants. They are well-studied metal-poor stars.

#### 3.1. Effective Temperatures

Colors available in the literature, used for derivation of effective temperatures  $T_{\text{eff}}$ , were taken from the following sources:  $J$ ,  $H$  and  $K$  in the TCS (Telescopio Carlos Sánchez) system from Alonso, Arribas & Martínez-Roger (1994, 1998); Strömgren  $ubvy\beta$  from the Catalogue by Hauck & Mermilliod (1998);  $V - I$  (Johnson or Cousins) and  $J$ ,  $H$  and  $K$  from the General Catalogue of Photometric Data (Mermilliod, Mermilliod & Hauck 1997). Transformations between different photometric systems were calculated using relations given by Bessell (1979), Bessell & Brett (1988) and Alonso et al. (1994, 1998).

The reddening values of most stars, estimated by using the maps of reddening by Burstein & Heiles (1982), were taken from Anthony-Twarog & Twarog (1994). Otherwise we adopted  $E(B-V) = 0$  for nearby stars (closer than  $d = 100$  pc) and  $E(B-V) = 0.03 \text{ csc } b [1 - \exp(-0.008 d(\text{pc}) \sin |b|)]$  (Bond 1980; see also Arenou et al. 1992) for stars with  $d > 100$  pc. Distances were determined from Hipparcos parallaxes (Perryman et al. 1997). The reddening corrections are small, typically  $E(B-V) \approx 0.07$ . The dereddened colors are given in Table 2.

Temperatures were determined using the  $V - I$ ,  $V - K$  and  $J - K$  calibrations of Lejeune, Cuisinier & Buser (1998, LCB98) and the same colors plus  $b - y$  for the calibrations of Alonso, Arribas & Martínez-Roger (1996a, 1999a, hereafter AAM99a). The mean  $T_{\text{eff}}$

of each calibration is shown in columns 2 (AAM99a) and 3 (LCB98) of Table 3. In a general way, both calibrations give similar values, but the calibrations of LCB98 show a larger standard deviation of temperatures from different colors ( $\sigma \approx 70$  K, against  $\sigma \approx 25$  K using AAM99a).

In Table 3 are also shown Infrared Flux Method (IRFM, column 4) temperatures, as determined by Alonso, Arribas & Martínez-Roger (1996b, 1999b, hereafter AAM99b). The calibration of AAM99a is based on their own IRFM temperature determinations, which explains the close values given under AAM99a and IRFM (AAM99b) in Table 3. The calibration of LCB98 is slightly cooler ( $-10$  K in the mean) than IRFM temperatures.

Means of  $T_{\text{eff}}$  values derived from colors (columns 2, 3 and 4 of Table 3) were checked against excitation equilibrium of Fe I lines. Literature equivalent widths of Fe I and Fe II (references in Sect. 3.3) were used.

The temperatures based on excitation equilibrium of Fe I are in the mean 40 K hotter than the mean of  $T_{\text{eff}}$  values derived from colors, and +50 K hotter in the mean relative to the IRFM temperatures (or +38 K if we consider the IRFM calibration of AAM99a). Note that Tomkin & Lambert (1999) found a similar result, with their Fe I temperatures being +45 K higher than those determined from the IRFM calibration of AAM99a. According to Tomkin & Lambert (1999), the small difference between Fe I temperatures and the IRFM temperatures is an indication that non-LTE effects are minor.

An example of the excitation equilibrium for HD 216143 is shown in Figs. 2a,b, where the individual iron abundances are plotted versus excitation potential and reduced equivalent width. No significant slope is seen in these Figs., indicating that  $T_{\text{eff}} = 4344$  K and  $v_t = 1.8 \text{ km s}^{-1}$  are adequate choices.

Two sets of  $T_{\text{eff}}$  values were adopted, those resulting from the excitation equilibrium (column 5 of Table 3) and those based on IRFM (column 4 of Table 3).

#### 3.2. Gravities

Nissen et al. (1997) and Allende Prieto et al. (1999) have shown that LTE spectroscopic gravities are systematically lower than trigonometric gravities derived from Hipparcos parallaxes in metal-poor stars. For this reason, both spectroscopic and trigonometric gravities were derived.

Spectroscopic gravities obtained by requiring ion-

<sup>3</sup><http://adsabs.harvard.edu>

ization equilibrium of Fe I and Fe II lines are given in Column 3 of Table 4. Hipparcos parallaxes  $\pi$  are used to derive trigonometric gravities, given in Column 7 of Table 4, where are also given the errors corresponding to the standard deviation  $\sigma(\pi)$ , which is of the order of 1 to 2 mas (a mean around 50% in  $\pi$ ). The errors in the trigonometric  $\log g$  are large for giants with  $\log g \lesssim 1.5$ , and small for dwarfs, in which case the gravities are also close to the spectroscopic values.

### 3.3. Metallicities

Equivalent widths of Fe I and Fe II from recent high resolution work in the literature (Kraft et al. 1992; Tomkin et al. 1992; Beveridge & Sneden 1994; Roe, Pilachowski & Armandroff 1994; Pilachowski, Sneden & Kraft 1996; Shetrone 1996; Tomkin & Lambert 1999; Fulbright 2000) were adopted. Optical spectra by Barbuy (1988) and Barbuy & Erdelyi-Mendes (1989) were used to check for any systematic error in the adopted equivalent widths. The present infrared spectra of the program stars, which contained a number of Fe I lines, were also used for a further check on [Fe/H]. The IR Fe I lines and respective equivalent widths are reported in Table 5.

MARCS model atmospheres by Bell et al. (1976) and Gustafsson et al. (1975) and OSMARCS by Edvardsson et al. (1993) were used for the calculations of curves of growth and spectrum synthesis. OSMARCS models were applied to 3 dwarf stars. The differences in [Fe/H] with respect to MARCS were  $\Delta[\text{Fe}/\text{H}](\text{OSMARCS-MARCS}) \leq 0.05$ . For the sake of consistency with the other sample stars, we assumed the results from MARCS models.

The adopted oscillator strengths for the optical iron lines are from the National Institute of Standards & Technology (Fuhr, Martin & Wiese 1988). For the infrared atomic lines we used the solar oscillator strengths determined in Meléndez & Barbuy (1999), which were derived adopting solar abundances from Grevesse, Noels & Sauval (1996). Curves of growth and abundances from equivalent widths of Fe I and Fe II were computed using the codes RENOIR and ABON by M. Spite.

In Table 7a are given the Fe abundances derived from (a) curves of growth of optical Fe I lines and checked with IR Fe I lines, obtained by adopting spectroscopic effective temperatures and gravities (columns 2 and 3 of Table 7a), (b) IRFM effective temperatures, Hipparcos gravities, and curves of growth based

on optical Fe II lines, and checked against the IR Fe I lines (columns 4 and 5 of Table 7a). Note that the agreement of the optical and IR-based Fe abundances shows that: a) there are no problems with the Phoenix data (such as scattered light) that might affect the equivalent widths which could cause the IR OH abundances to be low with respect to the UV OH, and b) there is no opacity problem, or other errors in the spectral code, between the optical and infrared regions.

Microturbulence velocities  $v_t$  were obtained from curves of growth and these values were checked by requiring no dependence of [Fe/H] against reduced equivalent width. The curve of growth for HD 216143, the most metal-poor star of the present sample, is shown in Figure 3.

The two sets of stellar parameters derived, and values from the literature are given in Table 4, where columns 2-5 show the spectroscopic parameters, columns 6-9 show the IRFM  $T_{\text{eff}}$ , trigonometric parallaxes and [Fe II/H], and literature values are given in columns 10-13.

### 3.4. Oxygen Abundances

The oxygen abundances were determined from fits of synthetic spectra to the sample spectra. The LTE code for spectrum synthesis described in Cayrel et al. (1991) was employed for the calculations.

The list of atomic lines present in the H band compiled by Meléndez & Barbuy (1999) was adopted, where oscillator strengths and damping constants were obtained from a line-by-line fitting of  $\approx 2,200$  lines in the infrared  $J$  and  $H$  bands, using the telluric-free solar spectrum atlas of Livingston & Wallace (1991) and Wallace, Hinkle & Livingston (1993). Hyperfine structure was also taken into account, as described in Meléndez (1999). Molecular lines of CN  $A^2\Pi - X^2\Sigma$ , CO  $X^1\Sigma^+$  (Meléndez & Barbuy 1999) and OH ( $X^2\Pi$ ) are included.

The infrared OH vibration-rotation lines ( $X^2\Pi$ ) used in this work are from the first-overtone ( $\Delta v = 2$ ) sequence. Laboratory line lists with wavenumbers and identifications were kindly provided by S. P. Davis. These line lists are from the work of Abrams et al. (1994). A few lines identified by Mélen et al. (1995), and a few theoretical lines (replacing unidentified lines) from Goldman et al. (1998) were also included. Energy levels for the OH lines were computed from molecular parameters given in Coxon &

Foster (1992) and Abrams et al. (1994). Molecular oscillator strengths were calculated from Einstein coefficients given in the extensive work by Goldman et al. (1998). A complete electronic version of line parameters for OH  $X^2\Pi$  transitions was kindly made available to us by A. Goldman. To our knowledge, Goldman et al. (1998) provide the most accurate Einstein values for infrared OH transitions available in the literature. The adopted dissociation potential is 4.392 eV (Huber & Herzberg 1979).

The main atomic and molecular features of the observed region are shown in Figure 1. The list of OH lines used for oxygen abundance determination, together with their molecular gf-values, energy levels and equivalent widths are given in Table 5.

The oxygen abundances derived show a dependence on the carbon abundances adopted. For 7 stars, carbon abundances were determined from the CO 3-0 bandhead ( $1.56\text{ }\mu\text{m}$ ) or from CO lines of the 2-0 and 3-1 bands ( $2.33\text{ }\mu\text{m}$ ), otherwise  $[\text{C}/\text{Fe}]$  values were taken from the literature.  $[\text{C}/\text{Fe}]$  values obtained from spectrum synthesis of the infrared CO bands are given in column 2 of Table 6. In the last column are given values from the literature, where most results are based on CH lines, except for the BC96 value for HD 103095 based on IR CO lines. The carbon abundances obtained from CO lines in the present work show good agreement with literature data.

Figures 4 and 5 show the fit of synthetic spectra to the observed spectra of HD 25329, the most metal-poor dwarf of our sample, and HD 37828, where the behavior of CO bands is illustrated.

The oxygen abundances derived from (a) spectroscopic parameters and (b) IRFM  $T_{\text{eff}}$ s, trigonometric gravities and  $[\text{Fe II}/\text{H}]$  are given in Table 7b. In Figures 6a,b are plotted  $[\text{O}/\text{Fe}]$  vs.  $[\text{Fe}/\text{H}]$  obtained from (a) spectroscopic parameters (open squares) and (b) IRFM temperatures, trigonometric gravities and  $[\text{Fe}/\text{H}]$  derived from Fe II lines (open triangles). Note that the uncertainty on trigonometric gravities cause a large dispersion on oxygen-to-iron ratios. We adopted as final result, the mean of methods (a) and (b), given in column 10 of Table 7b.

Adopting the spectroscopic parameters a mean oxygen-to-iron ratio of  $[\text{O}/\text{Fe}] \approx +0.52$  is obtained, whereas using the IRFM temperatures, Hipparcos gravities and  $[\text{Fe II}/\text{H}]$ ,  $[\text{O}/\text{Fe}] \approx +0.25$  is found. A mean of the two methods gives a final value of  $[\text{O}/\text{Fe}] \approx +0.38 \pm 0.2$  for the metallicity range of the sample

metal-poor stars of  $-2.2 < [\text{Fe}/\text{H}] < -1.2$ . Note that we have used Grevesse et al. (1996) abundance values, where  $\epsilon(\text{O}) = 8.87$ . If the Grevesse & Sauval (1998)  $\epsilon(\text{O}) = 8.83$  were used,  $[\text{O}/\text{Fe}]$  values would be higher by  $+ 0.04$  dex. The present oxygen abundances are in agreement with results from [O I] forbidden lines, which applies also to the 3 dwarfs of the present sample.

### 3.5. Errors

A check on the  $[\text{Fe}/\text{H}]$  values and possible systematic errors in the adopted equivalent widths was carried out by employing the high resolution optical spectra by Barbuy (1988) and Barbuy & Erdelyi-Mendes (1989). For five stars in common with the Lick, Texas and KPNO data, the Fe I equivalent widths  $W_\lambda$  were found to be about 10% smaller than those adopted; this difference is negligible since it implies a change in  $[\text{Fe}/\text{H}]$  of only 0.04 dex. A further check on  $[\text{Fe}/\text{H}]$  values was done with the infrared spectra observed in the present work, since five non-blended and other blended high excitation (5.5 to 6.5 eV) Fe I lines are observed in the region. The  $[\text{Fe}/\text{H}]_{\text{IR}}$  abundances determined by computing synthetic spectra (columns 3 and 5 of Table 7a) are in good agreement with the iron abundances from the analyses (columns 2 and 4 of Table 7a), within  $\Delta[\text{Fe}/\text{H}] \leq 0.15$ , and a mean difference  $\Delta[\text{Fe}/\text{H}] \approx +0.06$  and  $\Delta[\text{Fe}/\text{H}] \approx -0.15$  for parameters (a) and (b) (Sect. 3.3) respectively.

The errors due to uncertainties on  $T_{\text{eff}}$ ,  $\log g$  and  $v_t$  are inspected by computing the results for 3 sample stars. In Table 8 a mean of the errors for the giants HD 37828 and HD 216143, and those for the dwarf HD 103095 are given, where  $\Delta T_{\text{eff}} = 100\text{ K}$ ,  $\Delta \log g = 0.5\text{ dex}$  and  $\Delta v_t = 0.5\text{ km s}^{-1}$  are assumed.

### 4. Comments on UV OH lines

Using UV OH lines, both IGR98 and BKDV99 obtained high oxygen abundances in metal-poor stars, which appear to be in agreement with most results from permitted lines (but see Carretta et al. 2000). As already noted in Sect. 1, previous work on the UV OH lines resulted in lower oxygen abundances of  $[\text{O}/\text{Fe}] \approx +0.5$  to  $+0.6$  for metal-poor stars (Bessell, Sutherland & Ruan 1991; Nissen et al. 1994) in better agreement with the forbidden lines.

Let us analyse the possible sources of uncertainties in the use of the UV OH lines:

Nissen et al. (1994) transformed the Einstein  $A$  co-

efficients for the (0,0) transition calculated by Goldman & Gillis (1981) to molecular gf-values. In order to compute the same quantity for the (1,1) transition, Franck-Condon factors by Felenbok (1963) were adopted. Gillis et al. (2001) find results very similar to Goldman & Gillis (1981), and now include results for several ( $v'v''$ ) vibrational transitions. In order to fit the OH lines in the solar spectrum, Nissen et al. (1994) corrected the molecular gf-values by  $-0.16$  for the ( $v'v''$ ) = (0,0) and  $-0.49$  dex for the (1,1) vibrational transition. Calculations of Franck-Condon factors using the code by Jarmain & McCalum (1970) for the UV OH transitions (P.D. Singh, private communication), give values of  $q_{00} = 0.864$  and  $q_{11} = 0.683$ , or  $q_{11}/q_{00} = 0.79$ , the same ratio found from Felenbok (1963) results, whereas the ratio of molecular oscillator strengths  $gf(11)/gf(00) = 0.63$  following the new Einstein  $A$  coefficients by Gillis et al. (2001). With the corrections by Nissen et al. (1994), also adopted by BKDV99, this ratio becomes  $gf(11)/gf(00) = 0.37$ , much lower than that given in calculations of Franck-Condon factors.

IGR98 applied corrections on a OH line-by-line basis, in order to match the observed OH solar lines. Differences on gf-values employed by them, relative to Gillis et al. (2001) are down to  $-0.25$  dex (represented by asterisks in Fig. 7). In order to understand which may be the errors in IGR98's molecular gf-values, we computed the gf-values based on Goldman & Gillis (1981) and Gillis et al. (2001) and compared these values to IGR98's ones. In Figure 7 are plotted ratios of line-by-line molecular gf-values between different authors: (a) Gillis et al. (2001) relative to Goldman & Gillis (1981), which are essentially the same (filled circles); (b) theoretical values computed by IGR98 relative to Goldman & Gillis (1981), where unexpected differences are seen (open squares); (c) IGR98 values matched to the solar spectrum relative to Goldman & Gillis (1981), where IGR98 values are systematically lower (asterisks); (d) IGR98 adopted relative to theoretical values according to those authors (crosses). The IGR98 oxygen abundances would be lower by 0.1-0.2 dex if the original theoretical gf-values were used. Also in the sense of lowering further the oxygen abundances derived by IGR98, Asplund (2001a,b) suggested that calculations of UV OH lines would be more appropriate by taking into account 3-D model atmospheres, since these lines are very sensitive to temperature variations.

## 5. Discussion

A comparison of the present atmospheric parameters with literature values is given in Table 4 and oxygen abundances available from [OI], OI, UV OH and IR OH lines for the sample stars are reported in Table 9.

*[OI] lines:* The oxygen abundances obtained in the present work are in agreement with those derived from the [OI] line, and in a general agreement with values based on the forbidden [OI] lines given in the literature, which give a mean of  $[O/Fe] \approx 0.4$  to  $0.6$  in the metallicity range  $-2.5 < [Fe/H] < -1.2$  (see references in Sect. 1).

*OI triplet lines:* A discrepancy is seen between the presently derived O abundances from IR OH lines, together with those from the [OI] lines, with respect to those based on the permitted OI triplet lines. In order to try to solve this well-known discrepancy, King (1993) and Carretta et al. (2000) adopted higher effective temperature scales, which lower the [O/Fe] ratios deduced from the O I triplet bringing these into agreement with the values obtained from the [O I] lines. For HD 103095 the effective temperature of  $T_{\text{eff}} = 5132$  K adopted by BKDV99, in the King scale, bring all oxygen abundance indicators into agreement. It implies an increase of  $+100$  K in  $T_{\text{eff}}$  relative to the temperatures obtained from both Fe I and the IRFM. Note that recent high resolution spectroscopic analyses of HD 103095 by BC96, Tomkin & Lambert (1999) and Fulbright (2000) present temperatures of  $T_{\text{eff}} \approx 5000 \pm 50$  K, in agreement with recent IRFM estimates of  $T_{\text{eff}} = 5029$  K (Alonso et al. 1996b). While an increase of  $+100$  K is required for this particular case, in other cases temperature differences of up to  $+400$  K are required to bring the oxygen abundances derived from the O I triplet into agreement with the values obtained from [O I] lines (see Cavallo et al. 1997).

In Figure 8a the [O/Fe] ratios obtained from the IR OH lines, [O I] and O I for the star HD 25329 are shown for a range of temperatures: the  $T_{\text{eff}}$  has to be raised by  $\Delta T_{\text{eff}} \approx +300/+350$  K, well above the most likely values, in order to find an agreement (or even higher if Hipparcos gravities are used), relative to the spectroscopic value. The gravity obtained by ionization equilibrium from such an increase of 300 K in  $T_{\text{eff}}$  for HD 25329, is of  $\log g \approx 5.5$  dex, which is in disagreement by  $\Delta \log g \approx +0.6$  dex with respect to the  $\log g$  value obtained from its Hipparcos parallax,

as shown in Figure 8b.

Other problems with these lines need further investigation: the O abundances from the O I triplet lines show a large scatter (see Fig. 4 of Mishenina et al. 2000 and Fig. 7 of Cavallo et al. 1997) and some  $T_{\text{eff}}$  dependence (see Fig. 8 of Tomkin et al. 1992 and Fig. 2 of Carretta et al. 2000). See further discussion on these lines in Cayrel (2001b), Kiselman (2001a,b), Asplund (2001a,b) and Lambert (2001).

*UV OH lines:* Only two sample stars had the UV OH lines analysed: for HD 6582 there is good agreement between the present IR OH values and IGR98. For HD 103095 differences of  $\Delta[\text{O}/\text{Fe}] = -0.32$  with respect to IGR98, and  $-0.14$  (King scale) and  $0.0$  (Carney scale) with respect to BKDV99 are found; these differences are small, and if the gf-values of IGR98 and BKDV99 were assumed to be the original ones by Gillis et al. (2001), essentially no discrepancy would appear. Therefore no discrepancy between oxygen abundances derived from UV OH and IR OH are seen in these two dwarfs. However, considering the entire samples of UV OH results by BKDV99, Boesgaard (2001a,b), García López et al. (2001a,b) and IGR98 on one hand, and IR OH results by Balachandran et al. (2001a,b) and the present results (see also Meléndez et al. 2001) on the other, a sizeable discrepancy is seen of the order of  $\Delta[\text{O}/\text{Fe}] \sim 0.5$  at  $[\text{Fe}/\text{H}] \sim -2.0$ , and still undefined for lower metallicities.

*IR OH lines:*  $[\text{O}/\text{Fe}]$  values derived from the IR OH lines as a function of  $T_{\text{eff}}$  are plotted in Fig. 9a, where neither any significant scatter nor  $T_{\text{eff}}$  dependence are seen. Oxygen abundance determinations from IR OH lines in the literature were available up to now only for the metal-poor star HD 103095 by BC96. They obtained  $[\text{O}/\text{Fe}] = +0.29$  dex for the halo dwarf HD 103095, in good agreement with the present result of  $[\text{O}/\text{Fe}] = +0.30$  (or  $+0.28$  if BC96 parameters are used). In Table 10 are given  $[\text{O}/\text{Fe}]$  values derived from the IR OH lines for HD 103095, by adopting six different model parameters from the literature, showing that the  $[\text{O}/\text{Fe}]$  value obtained is not very sensitive to the model atmosphere parameters. Balachandran et al. (2001a,b) obtained  $[\text{O}/\text{Fe}] \approx +0.4$  for 6 stars with metallicities  $-2.6 \leq [\text{Fe}/\text{H}] \leq -1.0$ , in agreement with the present work. For 3 stars with  $[\text{Fe}/\text{H}] = -2.6, -2.7$  and  $-3.0$ , they find  $[\text{O}/\text{Fe}] = +0.7, +0.7$  and  $+0.9$  respectively. It is also important to note that for the star BD+23 3130, their results are in agreement with UV OH results from IGR98 if the original molecular gf-values by Goldman

& Gillis (1981) are used, and with that obtained from the [OI] 6300 Å line by Cayrel et al. (2001a).

In Figure 9b the  $[\text{O}/\text{Fe}]$  values (in stars) of  $[\text{Fe}/\text{H}] < -1.2$  vs. gravity are plotted. Oxygen abundances do not seem depleted in these metal-poor field stars. This is not unexpected since, in a recent work, Gratton et al. (2000) studied the mixing along the red giant branch in 62 metal-poor field stars, where none of their more evolved *field* giants (about half of the sample) shows any sign of oxygen depletion.

In Figure 10 are shown the present  $[\text{O}/\text{Fe}]$  determinations compared with the chemical evolution models of CMBN99 and PT95. The former model presents predictions of abundances relative to iron for an extended range of metallicities ( $-4.0 < [\text{Fe}/\text{H}] < 0.0$ ). No instantaneous recycling is assumed, and two different sets of yields from massive stars, one from WW95 and the other from TNH96 are employed. Their  $[\text{O}/\text{Fe}]$  values show a slope with decreasing metallicity, which is more pronounced if TNH96 yields are assumed. Similar predictions are given for other  $\alpha$  elements such as Mg, S, Si, Ca, for which the WW95 yields seem more compatible with the observational data. For the present range of metallicities, both their models reproduce reasonably well the observed  $[\text{O}/\text{Fe}]$  ratios. It would be important to test the prediction of increasing  $[\text{O}/\text{Fe}]$  with decreasing metallicity by measuring IR OH lines in stars of lower metallicities ( $[\text{Fe}/\text{H}] < -2.5$ ). The PT95 models present two versions, assuming instantaneous or delayed production approximations, using both TNH96 and WW95 yields, and their mean value for the range of metallicities  $-2.5 < [\text{Fe}/\text{H}] < 0.0$  is consistent with the present data.

## 6. Conclusions

We obtained high-resolution infrared spectra in the H-band, in order to derive oxygen abundances from IR OH lines. In order to have a homogeneous set of stellar parameters we carried out detailed analyses using equivalent widths of iron lines from the Lick, Texas and KPNO groups.

The stellar parameters were derived with basis on two methods: (a) spectroscopic parameters and (b) effective temperatures derived from the Infrared Flux Method (IRFM), trigonometric gravities using Hipparcos parallaxes, and metallicities  $[\text{Fe}/\text{H}]$  based on curves of growth of Fe II. Using stellar parameters of set (a), a mean  $[\text{O}/\text{Fe}] = +0.52$  is found, with a pos-

sible slope giving higher oxygen-to-iron ratios with decreasing metallicities, whereas with set (b) a constant  $[O/Fe] = +0.25$  is obtained. A mean of the two methods gives  $[O/Fe] = +0.38$  (assuming  $\epsilon(O) = 8.87$  and  $\epsilon(Fe) = 7.50$ ).

In summary, the sample stars with metallicities in the range  $-2.2 < [Fe/H] < -1.2$  show  $[O/Fe] \approx 0.4 \pm 0.2$ , with no significant evidence for an increase of  $[O/Fe]$  with decreasing metallicity.

We are grateful to the PHOENIX team at Kitt Peak, especially to the instrument scientist Ken Hinkle. We thank J. Tomkin, C. Pilachowski and J. Fulbright for providing unpublished equivalent widths, and S. P. Davis and A. Goldman for sending electronic files with OH molecular data. We are also grateful to a very competent referee, who helped us to improve the original manuscript. We acknowledge partial financial support from FAPESP, CNPq and CNPq/CNRS. J.M. acknowledges the FAPESP PhD fellowship n° 97/00109-8. We have made use of data from the Hipparcos astrometric mission of the ESA.

## REFERENCES

Abia, C. & Rebolo, R. 1989, *ApJ*, 347, 186

Abrams, M. C., Davis, S. P., Rao, M. L. P., Engleman, R., Jr. & Brault, J. W. 1994, *ApJS*, 93, 351

Allende Prieto, C., García-López, R., Lambert, D.L. & Gustafsson, B. 1999, *ApJ*, 527, 879

Alonso, A., Arribas, S. & Martínez-Roger, C. 1994, *A&AS*, 107, 365

Alonso, A., Arribas, S. & Martínez-Roger, C. 1996a, *A&A*, 313, 873

Alonso, A., Arribas, S. & Martínez-Roger, C. 1996b, *A&AS*, 117, 227

Alonso, A., Arribas, S. & Martínez-Roger, C. 1998, *A&AS*, 131, 209

Alonso, A., Arribas, S. & Martínez-Roger, C. 1999a, *A&AS*, 140, 261 (AAM99a)

Alonso, A., Arribas, S. & Martínez-Roger, C. 1999b, *A&AS*, 139, 335 (AAM99b)

Anthony-Twarog, B. J. & Twarog, B. A. 1994, 107, 1577

Arenou, F., Grenon, M. & Gomez, A. 1992, *A&A*, 258, 104

Asplund, M. 2001a, Joint Discussion 8, *Highlights of Astronomy*, ASP, in press

Asplund, M. 2001b, *NARv*, in press

Balachandran, S. C., Carr, J. S. & Carney, B. W., 2001a, Joint Discussion 8, *Highlights of Astronomy*, ASP, in press

Balachandran, S. C., Carr, J. S. & Carney, B. W., 2001b, *NARv*, in press

Balachandran, S. C. & Carney, B. W. 1996, *AJ* 111, 946 (BC96)

Barbuy, B. 1988, *A&A*, 191, 121

Barbuy, B. & Erdelyi-Mendes, M. 1989, *A&A*, 214, 239

Bell, R. A., Eriksson, K., Gustafsson, B. & Nordlund, A. 1976, *A&AS*, 23, 37

Bessell, M. S. 1979, *PASP*, 91, 589

Bessell, M. S. & Brett, J. M. 1988, *PASP*, 100, 1134

Bessell, M. S., Sutherland, R. S. & Ruan, K. 1991, *ApJ*, 383, L71

Beveridge, C. R. & Sneden, C. 1994, *AJ*, 108, 285

Boesgaard, A. M., King, J. R., Deliyannis, C. P. & Vogt, S. S. 1999, *AJ*, 117, 492 (BKDV99)

Boesgaard, A. M. 2001a, Joint Discussion 8, *Highlights of Astronomy*, ASP, in press

Boesgaard, A. M. 2001b, *NARv*, in press

Bond, H. E. 1980, *ApJS*, 44, 517

Burstein, D. & Heiles, C. 1982, *AJ*, 87, 1165

Carretta, E., Gratton, R. G. & Sneden, C. 2000, *A&A*, 356, 238

Cavallo, R. M., Pilachowski, C. A. & Rebolo, R. 1997, *PASP*, 109, 226

Cayrel, R., Perrin, M.-N., Barbuy, B. & Buser, R. 1991, *A&A*, 247, 108

Cayrel, R., Anderson, J., Barbuy, B. et al. 2001a, *NARv*, in press

Cayrel, R., Anderson, J., Barbuy, B. et al. 2001b, Joint Discussion 8, *Highlights of Astronomy*, ASP, in press

Chiappini, C., Matteucci, F., Beers, T. C. & Nomoto, K. 1999, 515, 226 (CMBN99)

Clegg, R. E. S., Lambert, D. L. & Tomkin, J. 1981, *ApJ* 250, 262

Conti, P.S., Greenstein, J.L., Spinrad, H., Wallerstein, G. & Vardya, M.S. 1967, *ApJ*, 148, 105

Coxon, J. A. & Foster, S. C., 1992, *Can. J. Phys.*, 60, 41

Edvardsson, B., Andersen, J., Gustafsson, B., Lambert, D.L., Nissen, P.E. & Tomkin, J. 1993, *A&A*, 275, 101

Felenbok, P. 1963, *Ann. Ap.* 26, 393

Friel, E., Kraft, R. P., Suntzeff, N. B. & Carbon, D. F., 1982, *PASP* 94, 873

Fields, B. D. & Olive, K. A. 1999, *ApJ*, 516, 797

Fuhr, J. R., Martin, G. A. & Wiese, W. L. 1988, *J. Phys. Chem. Ref. Data* 17, Suppl. 4

Fulbright, J. P. 2000, *AJ*, 120, 1841

Fulbright, J. P. & Kraft, R. P. 1999, *AJ*, 118, 527

García-López, R. J., Israelian, G., Rebolo, R., et al. 2001a, Joint Discussion 8, Highlights of Astronomy, ASP, in press

García-López, R. J., Israelian, G., Rebolo, R., et al. 2001b, *NARv*, in press

Gillis, J. R., Goldman, A., Stark, G. & Rinsland, C. P. 2001, *JQSRT*, 68, 225

Goldman, A. & Gillis, J. R. 1981, *JQSRT*, 25, 111

Goldman, A., Shoenfeld, W. G., Goorvitch, D., Chackerman C. Jr., Dothe, H., Mélen, F., Abrams, M. C. & Selby, J. E. A. 1998, *JQSRT*, 59, 453

Gratton, R. G., Sneden, C., Carretta, E. & Bragaglia, A. 2000, *A&A*, 354, 169

Gratton, R. G. & Ortolani, S. 1986, *A&A*, 169, 201

Grevesse, N. & Sauval, J. 1994, in *IAU Coll. no. 146 on Molecules in the Stellar Environment*, ed. U. Joergensen, p. 196

Grevesse, N., Noels, A. & Sauval, J. 1996, in *ASP Conf. Ser.* 99, eds. S.S. Holt, G. Sonneborn, p. 117

Grevesse, N. & Sauval, A.J., 1998, *SSRv*, 85, 161

Gustafsson, B., Bell, R. A., Eriksson, K. & Nordlund, Å. 1975, *A&A*, 42, 407

Hauck, B. & Mermilliod, M. 1998, *A&AS*, 129, 431

Hinkle, K. H., Wallace, L. & Livingston, W. 1995, *Infrared Atlas of the Arcturus Spectrum (0.9 - 5.3μm)*, Astronomical Society of the Pacific, San Francisco

Hinkle, K. H., Cuberly, R., Gaughan, N., Heynssens, J., Joyce, R., Ridgway, S., Schmitt, P. & Simmons, J. E. 1998, *Proc. SPIE* 3354, 810

Huber, K. P. & Herzberg, G. 1979, *Constants of Diatomic Molecules*, Van Nostrand Reinhold, New York.

Israelian G., García López, R. J. & Rebolo, R. 1998, *ApJ* 507, 805 (IGR98)

Jarmain, W.R. & McCallum, J.C. 1970, *TRAPRB* (London, Ontario, Dept. Phys., Univ. Western Ontario)

King, J. R. 1993, *AJ*, 106, 1206

King, J. R. 2000, *AJ*, 120, 1056

Kiselman, D. 2001a, Joint Discussion 8, *Highlights of Astronomy*, ASP, in press

Kiselman, D. 2001b, *NARv*, in press

Kiselman, D. & Nordlund, A. 1995, *A&A*, 302, 578

Kneller, J.P., Steigman, G. & Walker, T.P. 2001, in preparation.

Kraft, R. P., Suntzeff, N. B., Langer, G. E., Carbon, D. F., Trefzger, C. F., Friel, E. & Stone, R. P. S., 1982, *PASP*, 94, 55

Kraft, R. P., Sneden, C., Langer, G. E. & Prosser, C. F. 1992, *AJ*, 104, 645

Lambert, D. L. 2001, Joint Discussion 8, *Highlights of Astronomy*, ASP, in press

Lejeune, T., Cuisinier, F. & Buser, R. 1998, *A&AS*, 130, 65 (LCB98)

Livingston, W. & Wallace, L. 1991, *An Atlas of the Solar Spectrum in the Infrared (1.1 to 5.4 μm)*, National Solar Obs., Tech. Rep. 91-001, Tucson, AZ

Mélen, F., Sauval, A. J., Grevesse, N., Farmer, C. B., Servais, Ch., Delbouille, L. & Roland, G. 1995, *J. Mol. Spectrosc.*, 174, 490

Meléndez, J. 1999, *MNRAS*, 307, 197

Meléndez, J. & Barbuy, B. 1999, *ApJS*, 124, 527

Meléndez, J., Barbuy, B. & Spite, F. 2001, *NARv*, in press

Mermilliod, J.-C., Mermilliod, M. & Hauck, B. 1997, *A&AS*, 124, 349

Mishenina, T. V., Korotin, S. A., Klochkova V. G. & Panchuk, V. E. 2000, *A&A*, 353, 978

Nissen, P. E., Gustafsson, B., Edvardsson, B. & Gilmore, G. 1994, A&A 285, 440

Nissen, P. E., Høg, E. & Schuster, W. 1997, in Hipparcos, Venice '97 (ESO SP-402), p. 225

Nissen, P., Primas, F. & Asplund, M. 2001, NARv, in press

Pagel, B. E. J. & Tautvaišienė, G. 1995, MNRAS, 276, 505 (PT95)

Perryman, M.A.C., Lindegren, L., Kovalevsky, J. et al. 1997, A&A, 323, L49

Pilachowski, C. A., Sneden, C. & Kraft, R. P. 1996, 111, 1689

Roe, H., Pilachowski, C. A. & Armandroff, T. 1994, BAAS, 26, 1482

Shetrone, M. D. 1996, AJ, 112, 1517

Sneden, C., Lambert, D.L. & Whitaker, R.W. 1979, ApJ, 234, 964

Sneden, C., Kraft, R. P., Prosser, C. F. & Langer, G. E. 1991, AJ 102, 2001

Sneden, C., Pilachowski, C.A. & VandenBerg, D.A. 1986, ApJ, 311, 826

Sneden, C. & Primas, F. 2001a, Joint Discussion 8, Highlights of Astronomy, ASP, in press

Sneden, C. & Primas, F. 2001b, NARv, in press

Spiesman, W. J. & Wallerstein, G. 1991, AJ, 102, 1790

Spite, M. & Spite, F. 1991, A&A 252, 689

Takeda, Y., Takada-Hidai, M., Sato, S., Sargent, W.L.W., Lu, L., Barlow, T.A. & Jugaku, J., 2001, astro-ph/0007007

Thielemann, F. K., Nomoto, K. & Hashimoto, M., 1996, ApJ, 460, 408 (TNH96)

Tomkin, J., Lemke, M., Lambert, D. L. & Sneden, C. 1992, AJ, 104, 1568

Tomkin, J. & Lambert, D. L. 1999, ApJ, 523, 234

VandenBerg, D. A. 1985, in Proceedings of the ESO Workshop no. 21, on 'Production and Distribution of C, N, O Elements', eds. I.J. Danziger, F. Matteucci, K. Kjær, p. 73

VandenBerg, D. A., Swenson, F. J., Rogers, F. J., Iglesias, C. A. & Alexander, D. R. 2000, ApJ, 532, 430

Walker, T. P., Steigman, G., Schramm, D. N., Olive, K. A. & Fields, B. 1993, ApJ, 413, 562

Wallace, L., Hinkle, K. & Livingston, W. 1993, An Atlas of the Photospheric Spectrum from 8900 to 13600  $\text{cm}^{-1}$  (7350 to 11230 Å), National Solar Obs., Tech. Rep. 93-001, Tucson, AZ.

Westin, J., Sneden, C., Gustafsson, B. & Cowan, J.J. 2000, ApJ, 530, 783

Woosley, S. E. & Weaver, T. A. 1995, ApJS, 101, 181 (WW95)

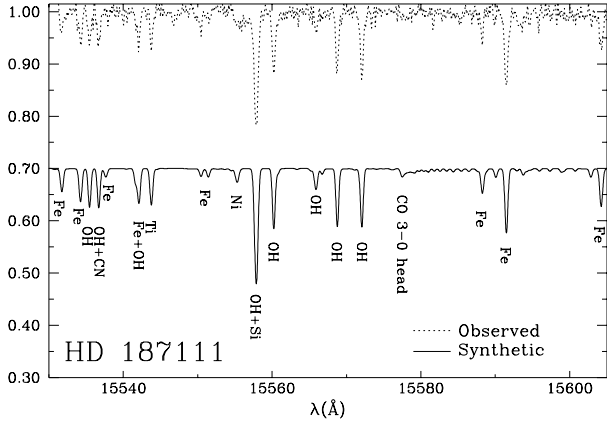


Fig. 1.— PHOENIX normalized spectrum of HD 187111 (upper spectrum) and synthetic spectrum with line identifications of atomic and molecular lines (lower spectrum).

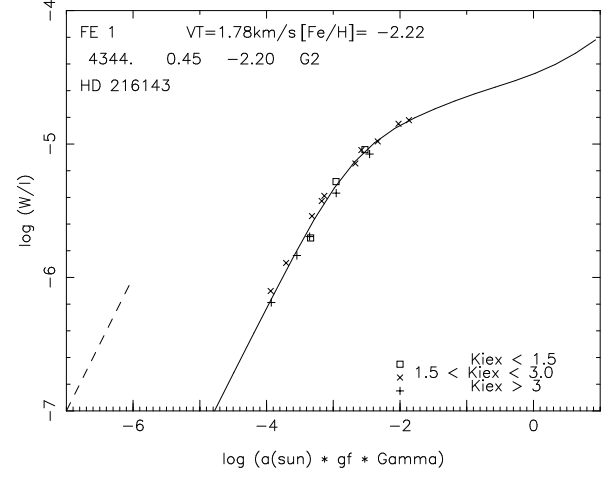


Fig. 3.— Curve of growth of Fe I for HD 216143.

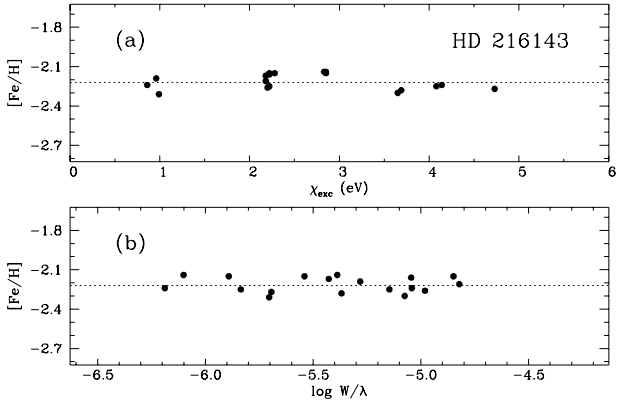


Fig. 2.— [Fe/H] vs. (a) excitation potential  $\chi_{exc}$  and (b) reduced equivalent width  $W/\lambda$  for the spectroscopic parameters of HD 216143. There is no significant trend with  $\chi_{exc}$  or  $\log W/\lambda$ .

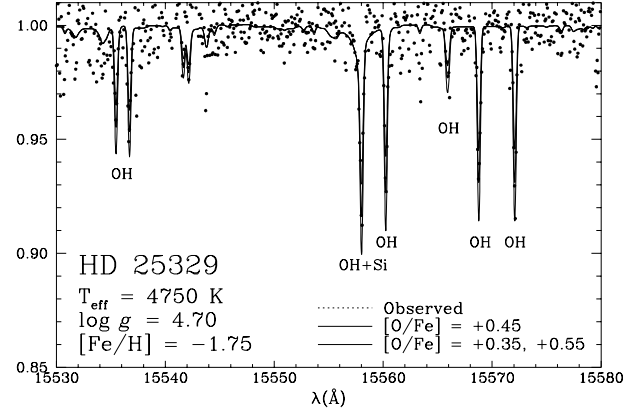


Fig. 4.— Spectrum of HD 25329 (dots) compared to synthetic spectra computed with  $[O/Fe]$ : +0.35, +0.45 (thick line) and +0.55.

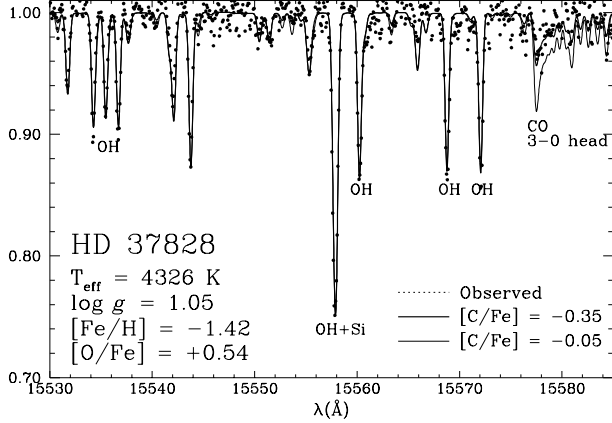


Fig. 5.— Observed spectrum of HD 37828 (dots) compared to synthetic spectra computed with  $[O/Fe] = +0.54$ ,  $[C/Fe] = -0.35$  (thick solid line) and  $[C/Fe] = -0.05$  (thin solid line).

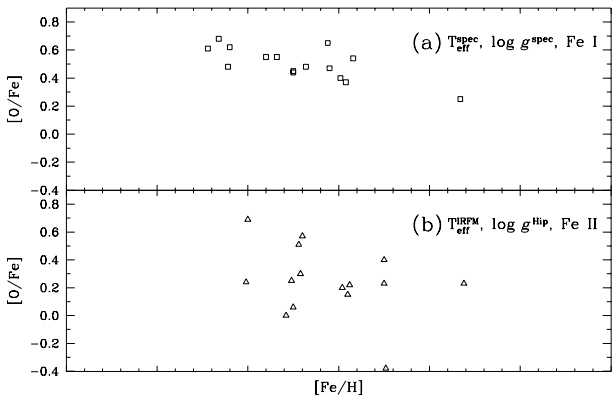


Fig. 6.—  $[O/Fe]$  vs.  $[Fe/H]$  from IR OH lines. (a) open squares correspond to results based on spectroscopic parameters; (b) open triangles give results from stellar parameters based on IRFM temperatures, trigonometric gravities and  $[Fe/H]$  derived from Fe II lines.

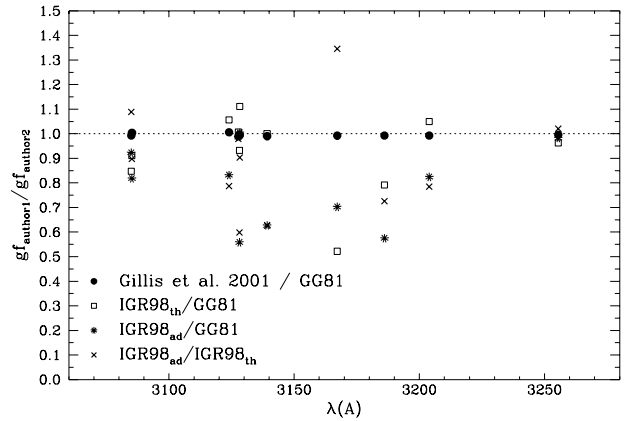


Fig. 7.— Ratios of molecular gf-values from different authors on a line-by-line basis: (a) Gillis et al. (2001) relative to Goldman & Gillis (1981), which are essentially the same (filled circles); (b) theoretical values computed by IGR98 relative to Goldman & Gillis (1981), where unexpected differences are seen (open squares); (c) IGR98 values fits to the solar spectrum relative to Goldman & Gillis (1981), where IGR98 values are systematically lower (asterisks); (d) IGR98 adopted relative to theoretical values according to IGR98 (crosses).

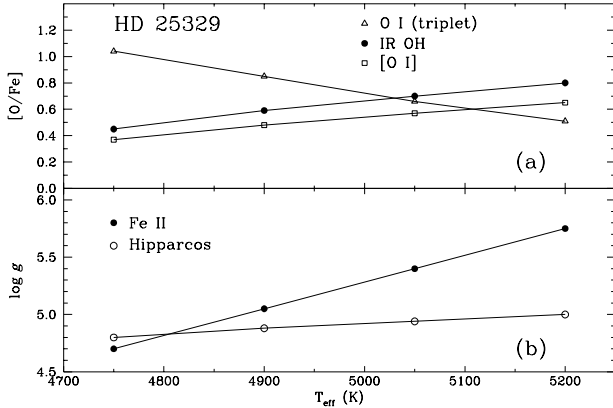


Fig. 8.— a)  $[O/Fe]$  vs.  $T_{\text{eff}}$  and  $\log g$  for HD 25329.  $T_{\text{eff}}$  (and correspondingly  $\log g$ ) has to be increased to bring the oxygen abundance from the IR OH lines (filled circles) and  $[O\text{ I}]$  (open squares) into agreement with the abundance derived from the O I triplet (open triangles). For  $[O\text{ I}]$  and O I the abundances were obtained from data by Spiesman & Wallerstein (1991) and Beveridge & Sneden (1994), respectively. b)  $\log g$  vs.  $T_{\text{eff}}$  for HD 25329 obtained from ionization equilibrium (filled circles) and Hipparcos parallaxes (open circles). Note that for  $T_{\text{eff}} \approx 4750 - 4800$  K (as obtained from Fe I and the IRFM) there is agreement between the gravities obtained from both methods.

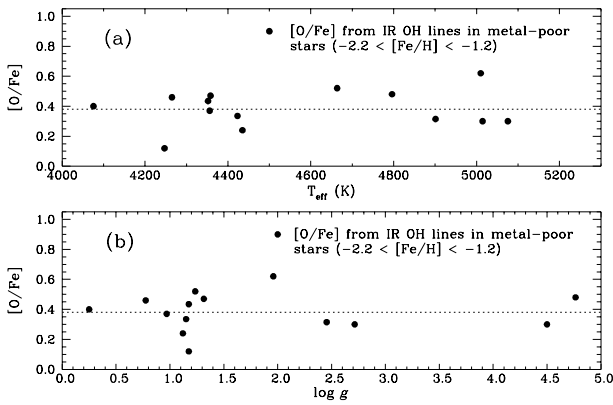


Fig. 9.—  $[O/Fe]$  from IR OH lines vs. (a)  $T_{\text{eff}}$  and (b)  $\log g$ , for stars with  $[\text{Fe}/\text{H}] < -1.2$ .

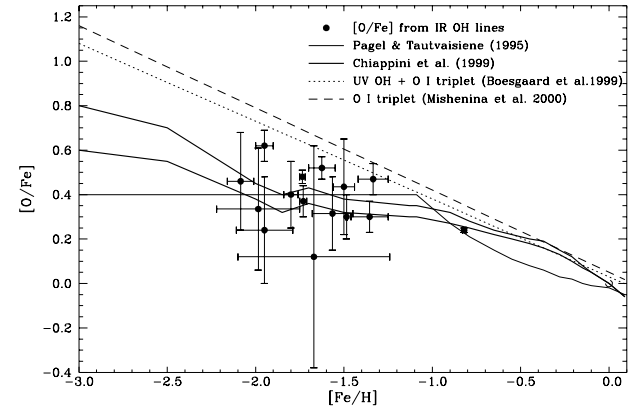


Fig. 10.— Comparison of oxygen abundances from IR OH lines (filled circles) with chemical evolution models. Fits of the average of the UV OH and OI triplet abundances by Boesgaard et al. (1999) (dotted line) and of the OI triplet abundances by Mishenina et al. (2000) (dashed line) are shown. Predictions of oxygen abundances from chemical evolution models by Chiappini et al. (1999) (thick line) and by Pagel & Tautvaišienė (1995) (thin line) are also plotted. The extremes of the error bars correspond to the (i) spectroscopic parameters and (ii) assuming IRFM  $T_{\text{eff}}$ s, trigonometric gravities and  $[\text{Fe II}/\text{H}]$  (see Sect. 3). The open circle represents the Sun.

TABLE 1  
LOG OF OBSERVATIONS

Star	V	Date (Sep. 1999)	Exposure (s)	S/N	band
HD 2665	7.7	26	3x1500	110	H
HD 6582	5.1	25, 27	3x600, 2x300	180, 100	H, K
HD 6755	7.7	25	4x1200	200	H
HD 21581	8.7	27	4x1800	100	H
HD 25329	8.5	25	6x1800	150	H
HD 26297	7.5	21	2x1200	130	H
HD 29574	8.3	21	2x1000	80	H
HD 37828	6.9	21, 26, 27	2x300, 2x300, 2x300	105, 105, 100	H, H, K
HD 165195	7.3	26	2x1500	200	H
HD 187111	7.7	26, 27	2x900, 2x1200	140, 150	H, K
HD 206739	8.6	27	3x1800	120	H
HD 216143	7.8	26	4x1800	230	H
HD 221170	7.7	25	4x1500	180	H
BD +060648	9.1	26	4x1800	180	H

TABLE 2  
COLORS

Star	$(b-y)_0$	$m_0$	$c_0$	$(V-I)_0^C$	$(V-I)_0^J$	$(J-K)_0^{TCS}$	$(V-K)_0^{TCS}$
HD 2665	0.502	0.067	0.340	1.166	1.500	0.530	2.092
HD 6582	0.437	0.205	0.213	—	—	0.443	1.833
HD 6755	0.474	0.095	0.290	0.854	1.097	0.518	1.988
HD 21581	0.527	0.117	0.331	0.943	1.212	0.546	2.189
HD 25329	0.528	0.303	0.155	0.988	1.270	0.557	2.305
HD 26297	0.738	0.237	0.607	—	—	0.713	2.845
HD 29574	0.931	0.219	0.721	—	—	0.806	3.368
HD 37828	0.694	0.308	0.491	1.190	1.530	—	—
HD 103095	0.484	0.222	0.155	0.871	1.120	0.492	2.054
HD 165195	0.821	0.120	0.701	1.286	1.653	0.749	2.936
HD 187111	0.754	0.197	0.588	—	—	0.770	2.917
HD 206739	0.602	0.172	0.446	—	—	0.603	2.413
HD 216143	0.677	0.150	0.569	—	—	0.653	2.617
HD 221170	0.713	0.114	0.547	—	—	0.685	2.692
BD +060648	0.787	0.175	0.577	—	—	0.740	2.932

NOTE.—C = Cousins, J = Johnson, TCS = Telescopio Carlos Sánchez

TABLE 3  
EFFECTIVE TEMPERATURES (K) BASED ON DIFFERENT METHODS (SECT. 3.1)

Star	AAM99a	LCB98	IRFM	Fe I
HD 2665	4964	4980	4990	5030
HD 6582	5295	5413	5315	5408
HD 6755	5053	5147	5008	5143
HD 21581	4869	4844	4870	4932
HD 25329	4777	4735	4842	4750
HD 26297	4324	4420	4322	4390
HD 29574	4047	4041	4020	4131
HD 37828	4390	4448	—	4326
HD 103095	5045	4924	5029	5000
HD 165195	4237	4229	4237	4293
HD 187111	4249	4200	4271	4433
HD 206739	4653	4609	4647	4680
HD 216143	4494	4433	4486	4360
HD 221170	4412	4348	4410	4460
BD +060648	4261	4217	4186	4308

TABLE 4

ADOPTED ATMOSPHERIC PARAMETERS OBTAINED FROM (A) SPECTROSCOPIC ANALYSIS (COLUMNS 2-5) AND (B) IRFM TEMPERATURES, TRIGONOMETRIC GRAVITIES AND [FE II/H] (COLUMNS 6-9), COMPARED WITH (C) LITERATURE VALUES (COLUMNS 10-14)

Star	(a) $T_{\text{eff}}^{\text{sp}}$	Spectroscopic $\log g^{\text{sp}}$	parameters $[\text{Fe}/\text{H}]^{\text{sp}}$	$v_t$	(b) $T_{\text{eff}}^{\text{IRFM}}$	IRFM, $\log g^{\text{Hip}}$	trigonometric $\log g^{\text{Hip}}$	$\log g$ and $[\text{Fe II}/\text{H}]$	Fe II $v_t$	(c) $T_{\text{eff}}$	Literature $\log g$	$[\text{Fe}/\text{H}]$	parameters $v_t$	ref.
HD 2665	5030	2.20	-1.90	1.4	4990		1.72±0.34	-2.00	1.4	5000	2.20	-1.97	1.3	1
										5050	2.20	-1.96	1.6	2
HD 6582	5408	4.40	-0.83	0.8	5315		4.52±0.00	-0.80	0.8	5250	4.40	-0.98	0.9	2
										5350	4.47	-0.92	1.0	3
HD 6755	5143	2.50	-1.49	1.4	5008		2.93±0.10	-1.48	1.4	5150	2.70	-1.57	1.4	1
										5150	2.80	-1.58	1.5	2
HD 21581	4932	2.20	-1.68	1.4	4870		2.71±0.25	-1.45	1.4	4825	2.00	-1.74	1.4	2
										4875	2.00	-1.74	1.5	4
HD 25329	4750	4.70	-1.75	0.7	4842		4.83±0.02	-1.72	0.7	4700	4.80	-1.85	1.3	2
										4775	4.71	-1.82	1.0	3
										4750	4.65	-1.78	0.5	5
										4750	4.70	-1.74	1.1	6
HD 26297	4390	1.00	-1.75	1.6	4322		0.94±0.93	-1.71	1.6	4400	1.10	-1.87	2.0	1
										4500	1.20	-1.73	1.7	2
										4450	1.20	-1.72	1.7	4
HD 29574	4131	0.20	-1.84	1.8	4020		0.30±0.82	-1.76	1.8	4100	0.00	-1.92	1.7	1
										4300	0.40	-1.88	1.7	2
										4280	0.22	-1.95	1.7	3
										4100	0.00	-1.93	1.6	7
HD 37828	4326	1.05	-1.42	1.3	4390		1.58±0.19	-1.25	1.3	4350	1.20	-1.42	1.4	7
HD 103095	5000	4.30	-1.46	1.1	5029		4.73±0.01	-1.25	1.1	4950	4.50	-1.46	0.7	2
										5040	4.31	-1.48	1.0	3
										5050	4.65	-1.22	1.4	8
HD 165195	4293	0.50	-2.17	1.7	4237		1.05±0.45	-2.01	1.7	4450	1.10	-2.24	1.9	1
HD 187111	4433	1.14	-1.56	1.6	4271		1.21±0.53	-1.44	1.6	4450	1.10	-1.71	1.9	2
										4400	1.08	-1.72	1.7	3
										4280	1.00	-1.67	1.5	7
										4250	0.70	-1.74	1.7	1
HD 206739	4680	1.50	-1.55	1.4	4647		0.97±0.89	-1.70	1.4	4675	1.70	-1.58	1.7	1
										4680	1.70	-1.58	1.5	4
HD 216143	4360	0.50	-2.22	1.8	4486		1.80±0.35	-1.75	1.8	4525	0.80	-2.18	1.8	1
										4525	1.00	-2.25	2.8	2
										4400	0.70	-2.26	1.8	7
HD 221170	4460	0.75	-2.11	1.6	4410		1.49±0.33	-1.79	1.6	4425	1.00	-2.15	1.5	1
										4500	0.90	-2.19	2.7	2
										4550	1.30	-2.10	2.0	7
BD +060648	4308	0.50	-2.10	1.7	4186		1.87±0.46	-1.24	1.7	4430	1.00	-2.11	1.8	7
										4500	1.10	-2.10	2.0	1

REFERENCES.—(1) Pilachowski et al. 1996; (2) Fulbright 2000; (3) Tomkin & Lambert 1999; (4) Kraft et al. 1992; (5) Beveridge & Sneden 1994; (6) Spiesman & Wallerstein 1991; (7) Shetrone 1996; (8) Balachandran & Carney 1996

TABLE 5  
EQUIVALENT WIDTHS OF IR OH AND Fe I LINES

OH,Fe I	$\lambda$ (Å)	$\chi_{exc}$ (eV)	log $gf$	1	2	3	4	5	6	7	8	9	10	11	12	13	14	15
3-1P1e5.5	15535.46	0.51	-5.23	-	-	-	-	11	26	24	37	-	24	38	10	11	13	12
3-1P1f5.5	15536.71	0.51	-5.23	-	-	-	-	-	25	22	-	-	-	37	-	-	14	-
2-0P2e10.5	15560.23	0.30	-5.31	4	4	7	10	24	54	75	70	18	50	56	-	24	20	36
4-2R2e,f2.5	15565.9	0.90	-5.00	-	-	-	-	11	-	21	20	-	13	20	-	-	-	12
2-0P1e11.5	15568.77	0.30	-5.27	3	6	5	11	26	51	76	68	14	46	56	20	22	20	40
2-0P1f11.5	15572.07	0.30	-5.27	7	5	5	12	26	50	73	66	18	49	58	20	26	-	39
Fe I	15534.26	5.64	-0.47	-	42	-	15	-	27	23	48	-	6	35	26	7	14	10
Fe I*	15550.45	6.34	-0.35	-	11	7	-	-	7	-	17	-	-	-	-	-	-	-
Fe I	15551.43	6.35	-0.31	-	13	7	-	-	7	-	19	-	-	8	-	-	-	-
Fe I*	15591.49	6.30	0.66	21	94	50	-	-	-	-	-	-	26	74	61	21	30	31
Fe I	15604.22	6.24	0.28	9	-	20	-	-	-	-	-	-	-	40	-	-	-	20

NOTE.—Identification of OH lines is given by their (v',v''), branch, and rotational quantum number J''. \* denotes blend of two Fe I lines.

REFERENCES.— (1) HD 2665 (2) HD 6582 (3) HD 6755 (4) HD 21581 (5) HD 25329 (6) HD 26297 (7) HD 29574 (8) HD 37828 (9) HD 103095 (10) HD 165195 (11) HD 187111 (12) HD 206739 (13) HD 216143 (14) HD 221170 (15) BD +060648

TABLE 6  
[C/FE] FROM CO LINES (SPECTROSCOPIC PARAMETERS) AND LITERATURE VALUES

Star	[C/Fe] <sub>CO</sub>	[C/Fe] <sub>lit</sub>
HD 2665		-0.30 <sup>1,2</sup>
HD 6582	+0.0	+0.04 <sup>3</sup>
HD 6755		-0.10 <sup>1,2</sup>
HD 21581		-0.40 <sup>2</sup>
HD 25329		+0.10 <sup>4</sup>
HD 26297	-0.2	
HD 29574	-1.0	<-1.0 <sup>2</sup>
HD 37828	-0.35	
HD 103095	-0.5	-0.32 <sup>5</sup> , -0.5 <sup>6</sup>
HD 165195		-1.00 <sup>1,6</sup>
HD 187111	-0.6	
HD 206739	-0.5	-0.50 <sup>1</sup>
HD 216143		-0.65 <sup>1</sup>
HD 221170		-0.30 <sup>1,6</sup>
BD +060648		-0.70 <sup>1,2</sup>

NOTE.—Solar abundances from Grevesse et al. (1996):  $\epsilon(\text{Fe}) = 7.50$  and  $\epsilon(\text{C}) = 8.55$  (in the scale  $\log(\text{X}/\text{H}) + 12$ )

REFERENCES.—(1) Kraft et al. 1982; (2) Friel et al. 1982; (3) Clegg, Lambert & Tomkin 1981; (4) Tomkin et al. 1992; (5) BC96; (6) Sneden, Pilachowski & Vandenberg 1986

TABLE 7A  
METALLICITIES OBTAINED FROM OPTICAL FE I, FE II LINES AND FROM INFRARED FE I LINES, USING (A)  
SPECTROSCOPIC PARAMETERS, (B) IRFM T<sub>eff</sub> AND TRIGONOMETRIC GRAVITIES.

Star	(a) T <sub>eff</sub> <sup>spec</sup> , [Fe/H] <sub>opt</sub>	log g <sup>Hip</sup> [Fe/H] <sub>IR</sub>	(b) IRFM T <sub>eff</sub> , [Fe II/H] <sub>opt</sub>	log g <sup>Hip</sup> [Fe/H] <sub>IR</sub>
HD 2665	-1.90	-1.88	-2.00	-1.91
HD 6582	-0.83	-0.93	-0.80	-0.95
HD 6755	-1.49	-1.39	-1.48	-1.42
HD 21581	-1.68	-1.66	-1.45	-1.69
HD 25329	-1.75	-	-1.72	-
HD 26297	-1.75	-1.64	-1.71	-1.67
HD 29574	-1.84	-1.83	-1.76	-1.92
HD 37828	-1.42	-1.27	-1.25	-1.23
HD 103095	-1.46	-	-1.25	-
HD 165195	-2.17	-2.19	-2.01	-2.29
HD 187111	-1.56	-1.51	-1.44	-1.59
HD 206739	-1.55	-1.47	-1.70	-1.48
HD 216143	-2.22	-2.17	-1.75	-2.17
HD 221170	-2.11	-1.92	-1.79	-1.97
BD +060648	-2.10	-1.96	-1.24	-2.03

TABLE 7B

OXYGEN ABUNDANCES FROM IR OH LINES: (A) SPECTROSCOPIC PARAMETERS, (B) IRFM  $T_{\text{eff}}$  , TRIGONOMETRIC GRAVITIES, FE II AND (C) MEAN VALUES

Star	(a) spectroscopic parameters [Fe/H] <sup>sp</sup>	[O/H] <sup>sp</sup>	[O/Fe] <sup>sp</sup>	(b) IRFM $T_{\text{eff}}$ , $\log g^{\text{Hip}}$ , Fe II [Fe II/H]	[O/H] <sup>Hip</sup>	$g^{\text{Hip}}$ , Fe II [O/Fe] <sup>Hip</sup>	(c) mean [Fe/H]	[O/H]	[O/Fe]
HD 2665	-1.90	-1.35	0.55	-2.00	-1.31	0.69	-1.95	-1.33	0.62
HD 6582	-0.83	-0.58	0.25	-0.80	-0.57	0.23	-0.82	-0.58	0.24
HD 6755	-1.49	-1.09	0.40	-1.48	-1.28	0.20	-1.49	-1.19	0.30
HD 21581	-1.68	-1.20	0.48	-1.45	-1.30	0.15	-1.57	-1.25	0.32
HD 25329	-1.75	-1.30	0.45	-1.72	-1.21	0.51	-1.74	-1.26	0.48
HD 26297	-1.75	-1.31	0.44	-1.71	-1.41	0.30	-1.73	-1.36	0.37
HD 29574	-1.84	-1.29	0.55	-1.76	-1.51	0.25	-1.80	-1.40	0.40
HD 37828	-1.42	-0.88	0.54	-1.25	-0.85	0.40	-1.34	-0.87	0.47
HD 103095	-1.46	-1.09	0.37	-1.25	-1.02	0.23	-1.36	-1.06	0.30
HD 165195	-2.17	-1.49	0.68	-2.01	-1.77	0.24	-2.09	-1.63	0.46
HD 187111	-1.56	-0.91	0.65	-1.44	-1.22	0.22	-1.50	-1.06	0.44
HD 206739	-1.55	-1.08	0.47	-1.70	-1.13	0.57	-1.63	-1.11	0.52
HD 216143	-2.22	-1.61	0.61	-1.75	-1.69	0.06	-1.99	-1.65	0.34
HD 221170	-2.11	-1.63	0.48	-1.79	-1.79	0.00	-1.95	-1.71	0.24
BD +060648	-2.10	-1.48	0.62	-1.24	-1.62	-0.38	-1.67	-1.55	0.12

TABLE 8

SENSITIVITY TO  $T_{\text{eff}}$  ,  $\log g$  AND  $v_t$  FOR GIANTS (A MEAN COMPUTED FOR HD 37828 AND HD 216143) AND DWARFS (COMPUTED FOR HD 103095).

Abundance	$\Delta T_{\text{eff}}$ +100 K	$\Delta \log g$ +0.5 dex	$\Delta v_t$ +0.5 km s <sup>-1</sup>	$(\Sigma x^2)^{1/2}$
Giants				
[FeI/H]	+0.13	+0.05	-0.15	0.20
[FeII/H]	-0.10	+0.22	-0.04	0.24
[O/H]	+0.20	-0.10	+0.03	0.23
[O/FeI]	+0.07	-0.15	+0.18	0.24
[O/FeII]	+0.30	-0.32	+0.07	0.44
Dwarfs				
[FeI/H]	+0.07	+0.01	-0.05	0.09
[FeII/H]	-0.03	+0.18	-0.01	0.18
[O/H]	+0.17	-0.03	+0.03	0.18
[O/FeI]	+0.10	+0.02	+0.08	0.13
[O/FeII]	+0.20	-0.15	+0.04	0.25

TABLE 9

[O/Fe] VALUES FROM THE LITERATURE COMPARED TO PRESENT RESULTS (MEAN VALUES ARE GIVEN, SEE SECT. 3)

Star	[O I]	O I	UV OH	IR OH	reference
HD 2665				0.62	1
	0.20	0.28			2
HD 6582				0.24	1
	0.45				3
		0.28			4
HD 6755				0.30	1
HD 21581				0.32	1
	0.29				5
	0.25				6
	0.39	0.32			2
HD 25329				0.48	1
	0.31				7
		1.07			8
HD 26297				0.37	1
	0.39				5
	0.25				6
	0.45				9
	0.31	0.41			2
HD 29574				0.40	1
	0.30				10
	0.50				6
HD 37828				0.47	1
	0.35				10
	0.32				11
HD 103095				0.30	1
	0.48				12
		0.89			13
	0.33	0.42		0.29	14
	0.37		0.62		4
		0.40	0.44		15 King scale
		0.61	0.29		15 Carney scale
	0.45	0.22			2
HD 165195				0.46	1
	0.59	0.61			16
	0.40				6
HD 187111				0.44	1
	0.34				5
	0.40				6
	0.34				7
	0.35				2
HD 206739				0.52	1
	0.25				5
	0.25				6
HD 216143				0.34	1
	0.16				10
	0.69				9
HD 221170				0.24	1
	0.22				5
BD +060648				0.12	1
	0.45				10

REFERENCES.—(1) This work; (2) Gratton et al. (2000); (3) Clegg et al. 1981; (4) IGR98; (5) Kraft et al. 1992; (6) Barbuy (1988); (7) Spiesman & Wallerstein 1991; (8) Beveridge & Sneden 1994; (9) Gratton & Ortolani 1986; (10) Shetrone (1996); (11) Barbuy & Erdelyi-Mendes (1989); (12) Spite & Spite (1991); (13) Tomkin et al. 1992; (14) BC96; (15) BKDV99; (16) Takeda et al. (2000).

TABLE 10  
[O/FE] RATIOS FOR HD 103095 USING DIFFERENT MODEL PARAMETERS

Model atmosphere $T_{\text{eff}}$ , $\log g$ , [Fe/H], $v_t$ , reference	IR OH	UV OH	[O I]	O I
5000 K, 4.30, $-1.46$ , $1.1 \text{ km s}^{-1}$ , 1a	+0.37	—	+0.31	+0.60
5029 K, 4.73, $-1.25$ , $1.1 \text{ km s}^{-1}$ , 1b	+0.23	—	+0.34	+0.50
5040 K, 4.65, $-1.22$ , $1.4 \text{ km s}^{-1}$ , 2	+0.28	—	+0.28	+0.42
5030 K, 4.55, $-1.30$ , $1.0 \text{ km s}^{-1}$ , 3	+0.28	+0.62 <sup>3</sup>	+0.29	+0.48
5005 K, 4.65, $-1.37$ , $1.5 \text{ km s}^{-1}$ , 4	+0.30	+0.29 <sup>4</sup>	+0.37	+0.62
5132 K, 4.75, $-1.26$ , $1.5 \text{ km s}^{-1}$ , 5	+0.39	+0.44 <sup>5</sup>	+0.37	+0.40

NOTE.—Oxygen abundances based on IR OH lines, [O I] and O I lines were derived using data by BC96, Spite & Spite (1991) and Tomkin et al. (1992), respectively. For the UV OH lines the [O/Fe] ratios are reported as given in IGR98 and BKDV99

REFERENCES.—(1) This work; (2) BC96; (3) IGR98; (4) BKDV99 (Carney scale); (5) BKDV99 (King scale)